

# Influence of mineral admixtures on the mechanical property and durability of waste oyster shell mortar

Liao Yingdi<sup>1,2,3</sup> Wang Xin<sup>1</sup> Feng Jiarui<sup>1,4</sup> Meng Yanting<sup>1</sup> Chen Da<sup>1,2,3</sup> Da Bo<sup>1,2,3</sup>

(<sup>1</sup>College of Harbour, Coastal and Offshore Engineering, Hohai University, Nanjing 210098, China)

(<sup>2</sup>Key Laboratory of Coastal Disaster and Defence of Ministry of Education, Hohai University, Nanjing 210098, China)

(<sup>3</sup>Yangtze Institute for Conservation and Development, Hohai University, Nanjing 210098, China)

(<sup>4</sup>Nanjing R&D High-Tech Co. Ltd., Nanjing 210024, China)

**Abstract:** To mitigate the environmental pollution caused by aquatic waste, crushed waste oyster shell (WOS) was added as an aggregate to the mortar. The impact of varying dosages (0%, 20%, 30%, and 40%) of fly ash (FA)/slag powder (SG) and curing periods on the workability, mechanical properties, and durability of the resulting mixtures were investigated. Furthermore, the ecological and economic benefits of WOS mortars were examined. The findings reveal that the compressive strength and static modulus of elasticity in WOS mortar decreased moderately after adding the mineral admixture during the initial curing phase. However, the mechanical properties of WOS mortar improved upon extending the curing period. Additionally, the partial replacement of cement with FA/SG promoted the migration ability of chloride and minimized the drying shrinkage in WOS mortars. In scenarios where engineering application requirements are satisfied, the utilization of WOS mortar could reduce CO<sub>2</sub> emissions by 29%.

**Key words:** crushed waste oyster shell (WOS) mortar; workability; mechanical property; durability; ecological and economic benefits

**DOI:** 10.3969/j.issn.1003-7985.2023.03.008

Globally, cementitious material has become a ubiquitous component in construction, with the annual consumption of cement-based materials projected to escalate to approximately  $1.8 \times 10^{10}$  t by 2050<sup>[1]</sup>. Consequently, the pervasive application of these materials can exert a considerable impact on the environment<sup>[2]</sup>. Considering the increasing utilization of cement-based construction, the necessity to develop ecofriendly, affordable, and high-performance alternatives for natural aggregates is imminent for addressing the continual depletion of

natural resources and protecting the environment against pollution. The waste oyster shells (WOS) generated in the aquaculture sector, known for their high calcium carbonate content, have created a substantial environmental dilemma owing to their large-scale disposal. Nonetheless, WOS is a promising substitute for natural river sand, attributed to its similar physical and chemical properties<sup>[3]</sup>.

Numerous studies have explored the application of WOS in mortar or concrete. Mortars comprising 20% crushed WOS fine aggregate possess higher compressive strengths and reduced water absorption than full-river-sand mortar<sup>[4]</sup>. Owing to the filling function of WOS fine aggregate, its integration with fine particles has been recommended within construction materials; these materials demonstrate elevated compressive strength when paired with fine WOS, as opposed to coarse WOS<sup>[5]</sup>. Thus, WOS exhibits substantial potential for the partial replacement of natural river sand.

Previous research on standard concrete reported that the judicious application of supplementary cementitious materials such as fly ash (FA) or slag powder (SG) for partial cement replacement can enhance the workability of fresh concrete<sup>[6]</sup>, in addition to the strength and durability of hardened concrete. Regrettably, studies investigating the influence of FA and SG as supplementary cementitious materials on the fresh and engineering properties of WOS mortars are scarce.

This study employed two industrial byproducts (FA and SG) as supplementary cementitious materials for partial cement replacement and formulated WOS mortars with four substitution ratios (0%, 20%, 30%, and 40%). Initially, we examined the workability of WOS mortars with varying FA and SG replacements. Subsequently, the mechanical properties were assessed, and the durability was ascertained. Finally, the ecological and economic benefits of WOS mortars were analyzed.

## 1 Experiment

### 1.1 Materials

This study employed ordinary Portland cement (OPC) according to the standard ASTM C 150. The chemical composition of the OPC was determined in accordance

**Received** 2023-04-15, **Revised** 2023-07-30.

**Biographies:** Liao Yingdi (1977—), female, doctor, associate professor, liaoyingdi@hhu.edu.cn; Da Bo (corresponding author), male, doctor, associate professor, dabobo@hhu.edu.cn.

**Foundation items:** The National Natural Science Foundation of China (No. 51509081, 52208241), Jiangsu Provincial Key Research and Development Program (No. BE2020715).

**Citation:** Liao Yingdi, Wang Xin, Feng Jiarui, et al. Influence of mineral admixtures on the mechanical property and durability of waste oyster shell mortar[J]. Journal of Southeast University (English Edition), 2023, 39(3): 277 – 283. DOI: 10.3969/j.issn.1003-7985.2023.03.008.

with BS EN 197-1, and its mineral composition is delineated in Tab. 1. The specific gravity and surface area of the OPC were measured to be  $3.01 \text{ g/cm}^3$  and  $3520 \text{ cm}^2/\text{g}$ , respectively. The FA and SG were used as supplementary cementitious materials. The FA, in compliance with ASTM C 618, was sourced from a coal-fired power plant, while the SG was supplied by a cast-iron factory in China. The chemical compositions of both FA and SG are presented in Tab. 1.

River sand (fineness modulus 1.63, saturated surface-

dry water absorption 0.87%, apparent density  $2620 \text{ kg/cm}^3$ , bulk density  $1540 \text{ kg/cm}^3$ , and void fraction 41%) derived from China, and crushed WOS (fineness modulus 3.66, saturated surface-dry water absorption 6.84%, apparent density  $2411 \text{ kg/cm}^3$ , bulk density  $1354 \text{ kg/cm}^3$ , and void fraction 44%) obtained from the northern coast of China were used as fine aggregates (see Fig. 1). In this mixture, a naphthalene-based superplasticizer was used as a water reducer.

**Tab. 1** Chemical and mineral composition of the cementitious materials

Materials	Chemical composition/%								Mineral composition/%			
	SiO <sub>2</sub>	Al <sub>2</sub> O <sub>3</sub>	CaO	Fe <sub>2</sub> O <sub>3</sub>	MgO	SO <sub>3</sub>	K <sub>2</sub> O	Na <sub>2</sub> O	C <sub>3</sub> S	C <sub>2</sub> S	C <sub>3</sub> A	C <sub>4</sub> AF
Cement	21.35	4.94	60.16	2.71	0.46	1.96	0.48	1.00	60.74	16.18	6.66	14.17
FA	56.79	28.21	3.00	5.31	5.21	0.68	1.34	0.45				
SG	34.62	11.82	37.73	2.73	9.43	1.42	0.50	0.35				

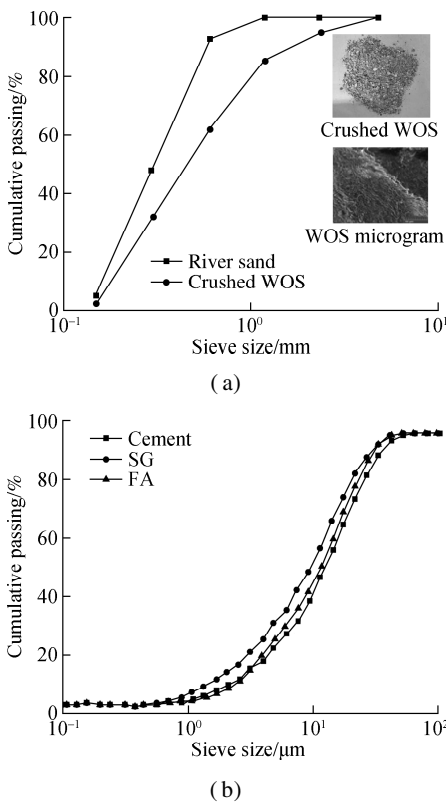


**Fig. 1** Grading curves of aggregates and cementitious materials. (a) Aggregates; (b) Cementitious materials

## 1.2 Mixture proportions

In this study, the content of cementitious materials (cement, FA, and SG) within the mortar was uniformly set at  $608 \text{ kg/m}^3$ , and the water-cement ratio was maintained at 0.45. Furthermore, WOS served as a substitution for 30% of river sand<sup>[7-8]</sup>. During the mortar mixing process, the replacement rates by FA or SG for cement were segmented into four stages: 0%, 20%, 30%, and 40% (with FA-20 and SG-20 symbolizing mortars containing 20% FA and 20% SG, respectively). The dosage of the water reducer was set at 0.25% of the total cementitious materials. Tab. 2 provides a comprehensive outline of the mixed proportions for the mortar specimens.

## 1.3 Testing procedures

### 1.3.1 Workability

Workability assessments of the mortars were conducted according to BS EN 1015-3 to measure the initial slump flow by averaging the diameters of fresh mortar on the flow table in two vertical directions. Subsequent inspection of the slump flow value of the mortar was conducted at intervals of 30, 60, 90, and 120 min after the initial test.

**Tab. 2** Mix proportions of the mortar specimens

Sample	$\rho(\text{cement})/$ ( $\text{kg} \cdot \text{m}^{-3}$ )	$\rho(\text{FA})/$ ( $\text{kg} \cdot \text{m}^{-3}$ )	FA replacement rate/%	$\rho(\text{SG})/$ ( $\text{kg} \cdot \text{m}^{-3}$ )	SG replacement rate/%	$\rho(\text{WOS})/$ ( $\text{kg} \cdot \text{m}^{-3}$ )	$\rho(\text{river sand})/$ ( $\text{kg} \cdot \text{m}^{-3}$ )
OPCM	608						1520
WOSM-control	608						
WOSM-F20	486.4	121.6	20				
WOSM-F30	425.6	182.4	30				
WOSM-F40	364.8	243.2	40			456	1064
WOSM-SG20	486.4			121.6	20		
WOSM-SG30	425.6			182.4	30		
WOSM-SG40	364.8			243.2	40		

### 1.3.2 Mechanical property

Considering the mechanical properties, the mortars were analyzed for compressive strength following ASTM C 349 and static modulus of elasticity ( $E$ ) following ASTM C 469. The mortar samples for compressive strength testing were machined at dimensions of 40 mm  $\times$  40 mm  $\times$  160 mm. The value of  $E$  was gaged using servo-controlled uniaxial testing equipment on mortar cylinders measuring  $\Phi$ 50 mm  $\times$  100 mm (see Fig. 2). The value of  $E$  was extracted from the slope of the stress-strain curve at 1/3 of the peak stress.

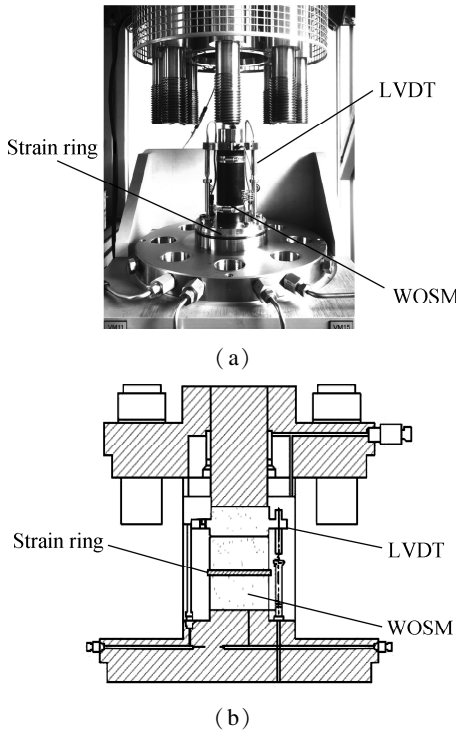


**Fig. 2** Auto-compensated and auto-equilibrated triaxial test systems. (a) Actual diagram; (b) Schematic diagram

### 1.3.3 Durability

The mortar durability was evaluated based on factors such as drying shrinkage (in line with ASTM C 157) and chloride migration coefficient (compliant with NT BUILD 492). The samples designated for drying shrinkage tests comprised separate sections of mortar, each subjected to individual testing. These drying shrinkage tests were conducted across 1, 4, 7, 14, 28, 56, and 90 d after the initial length measurements of the demolded samples using a length comparator.

Furthermore, cylinder samples ( $\Phi$ 100 mm  $\times$  50 mm) prepared for the chloride migration test were positioned within a standard curing box, regulated at a temperature of  $(20 \pm 3)^\circ\text{C}$  and relative humidity of  $(95 \pm 5)\%$ , and cured until the required age of 28 and 90 d was reached.

## 2 Results and Discussion

### 2.1 Workability

The variations in the slump flow of WOS mortars with

FA and SG are depicted in Fig. 3. The observations confirmed that the incorporation of WOS tends to adversely affect the workability of the mortar. This can be ascribed to the elevated water absorption of crushed WOS under the dry conditions of the saturated surface compared to the river sand. Concurrently, the nonuniform shape of the crushed WOS within the mortar intensified the friction at the aggregate-mortar interface. For WOS mortars, consistent reductions in the slump flow were recorded over time, whereas the initial slump flow ascended in response to the increased substitution ratios of both FA and SG. The peak slump flow values were achieved with a 40% substitution ratio for FA and SG. In contrast, to control mortars, the growth rates of initial slump flow values are approximately 2.75%, 5.29%, 7.03% for FA and 1.74%, 3.22%, 5.76% for SG, at substitution ratios of 20%, 30%, and 40%, respectively. Laskar et al.<sup>[9]</sup> interpreted this phenomenon as a result of the spherical shape of FA, which enlarges the mortar's surface area, diminishes fine aggregate-to-mortar friction, and improves lubrication, thus enhancing mortar liquidity. Zhang et al.<sup>[10]</sup> posited that the dissolution of  $\text{OH}^-$  ions from cement particles during early hydration imparts an electrical charge to the mortar, producing a flocculation structure and entrapping water. The addition of SG to the surface of cement, along with certain superfine SG particles, disrupts the flocculation structure, liberates the entrapped moisture, fosters a dispersion effect, and consequently improves fluidity. Notably, the fluidity of mortar with FA surpasses that with SG.

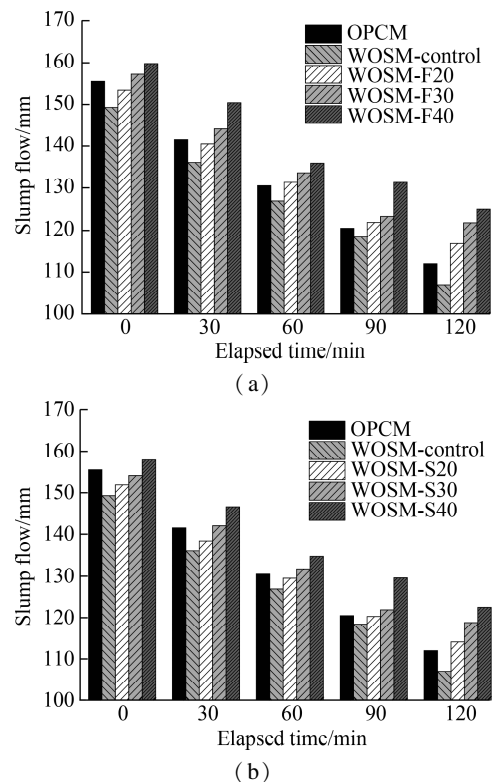


**Fig. 3** Variations in slump flow of WOS mortars with FA and SG. (a) FA; (b) SG

## 2.2 Mechanical property

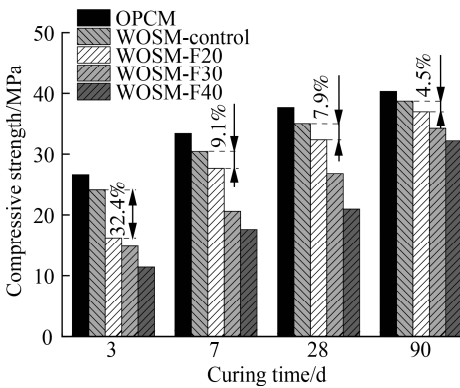
### 2.2.1 Compressive strength

Fig. 4 portrays the variations in the compressive strength of WOS mortars with FA and SG. As observed, the WOS mortars displayed a lower compressive strength than the OPC mortars (without WOS). This may be attributed to the needle-like particle structure of crushed WOS that offers high friction resistance, resulting in small slump and expansion. Moreover, owing to the low strength of the WOS, the WOS mortar displays a lower strength than the OPC mortar. Additionally, the increasing substitution ratios of FA and SG contribute to a decline in the compressive strength of the WOS mortars, specifically at the initial curing stage. For instance, WOS mortars with 40% FA at 28 and 90 d achieved approximately 60% and 83% strength of the control mortars, similar to that in WOS mortars with SG. In contrast, the WOS mortar with 20% FA displayed 32% and 4%, and that with 20% SG exhibited 19% and 3% strength of the WOS mortar at 3 and 90 d, respectively. The data revealed that the strength of WOS mortars with FA and SG accelerates more rapidly than that of WOS mortars without FA and SG, and this disparity in strength decreases as the curing period extends. The constructive impact of SG on compressive strength surpasses that of FA, owing to the slower pozzolanic reaction activities of FA and SG

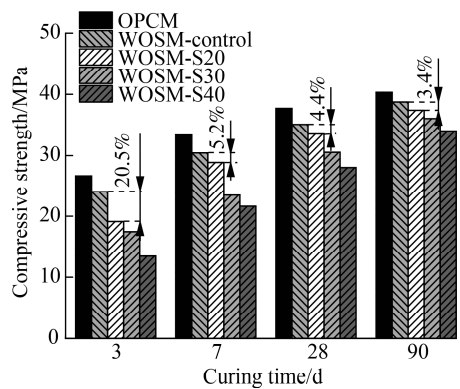
during the early curing phase, thereby relatively decreasing the compressive strength. However, at the later stages, FA and SG react with  $\text{Ca}(\text{OH})_2$  emanating from primary hydration<sup>[11–12]</sup>. Both these trends can be explained based on the delay in the formation of calcium-silicate-hydrate (C-S-H) because the pozzolanic reaction emerges as the major reaction with the increasing replacement of the cement content<sup>[13]</sup>. Consequently, the difference in the compressive strength between the control mortar and the WOS mortar with FA/SG decreased with the curing age.

### 2.2.2 Static modulus of elasticity

Fig. 5 displays the variation of the static modulus of elasticity of WOS mortars in relation to FA and SG. As observed, the incorporation of WOS marginally decreased the  $E$  value of the mortar samples. However, this reduction in  $E$  for WOS mortar can be mitigated by extending the curing period, a phenomenon that aligns with the compressive strength, given its inherently low nature. Moreover, the WOS mortars with FA and SG demonstrate a lower  $E$  compared to the WOS-Control mortar. As FA and SG increased, the  $E$  of WOS mortars declined correspondingly. Relative to the WOS-Control mortar, the 90-d  $E$  of WOS mortars with FA at 20%, 30%, and 40% decreased by 7.69%, 10.00%, and 11.54%, respectively, whereas that of WOS mortars with SG at 20%,

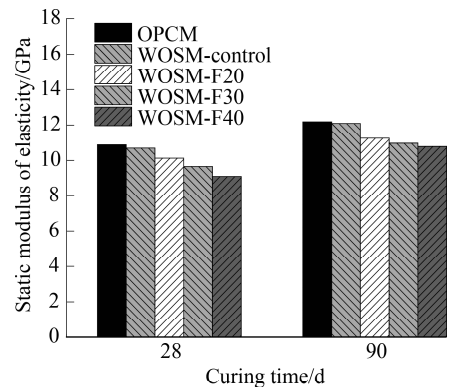


(a)

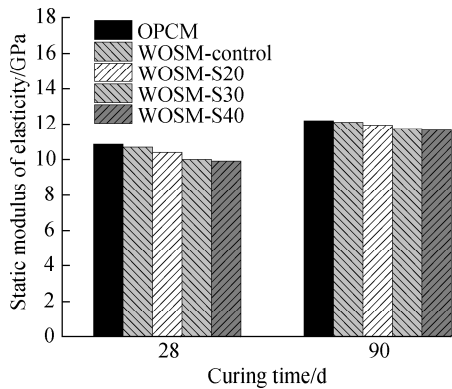


(b)

**Fig. 4** Variations in compressive strength of WOS mortars with FA and SG. (a) FA; (b) SG



(a)



(b)

**Fig. 5** Variation of the static modulus of elasticity of WOS mortars with FA and SG. (a) FA; (b) SG

30%, and 40% decreased by 2.07%, 3.64%, and 4.43%, respectively. Notably, under identical conditions, the WOS mortar with FA consistently exhibited a lower  $E$  than the WOS mortar with SG. These findings suggest that WOS mortars with 20% SG can attain nearly the same  $E$  as the control mortar during the later stages of curing.

## 2.3 Durability

### 2.3.1 Drying shrinkage

The variations in the drying shrinkage of WOS mortars with FA and SG are presented in Fig. 6. The evidence confirms that the integration of WOS improved the drying shrinkage of the mortar samples. This phenomenon may be attributed to the water absorption capacity of the crushed WOS (6.84%), which is considerably higher than that of natural river sand (0.87%), resulting in elevated moisture content within the internal pores of the mortar. Additionally, the reduced hardness of crushed WOS<sup>[14]</sup> may contribute to the greater drying shrinkage of WOS mortars. At the commencement of curing, the drying shrinkage of WOS mortars across various groups appears remarkably similar. Furthermore, the drying shrinkage proliferates with the progression of curing time, yet the growth rate of drying shrinkage diminishes as curing time extends.

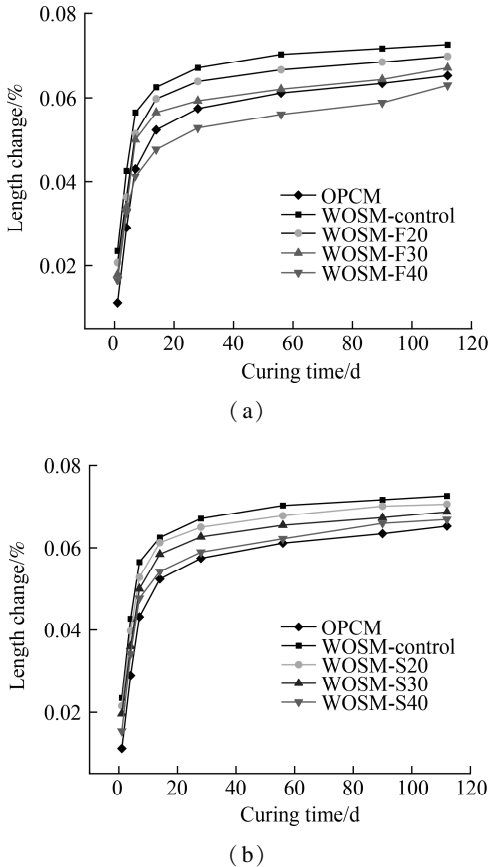


**Fig. 6** Variations in drying shrinkage of WOS mortars with FA and SG. (a) FA; (b) SG

The incorporation of FA and SG serves to curtail the hydration degree of cement, contract the pore volume of WOS mortar, and increase the deformation resistance of WOS mortar. Conversely, the powder functions directly as a microfiller, abating voids and furnishing skeletal support to counteract deformation. Additionally, the hydration and pozzolanic reactions consume substantial amounts of free water, leading to a decrease in evaporative water content, which ultimately diminishes the drying shrinkage. Consequently, by employing FA and SG in suitable proportions, the shrinkage of WOS mortar can be effectively reduced, and the occurrence of shrinkage cracking in WOS mortar can be averted during the hardening process.

### 2.3.2 Chloride migration coefficient

Fig. 7 elucidates the variation in the chloride migration coefficient of WOS mortars in association with FA and SG. The findings reveal that the introduction of crushed WOS into the mortar enhances the likelihood of chloride migration. This implies that as the content of WOS is augmented, the resistance to chloride ion penetration correspondingly diminishes. This phenomenon might be attributed to the presence of crushed WOS, which results in an increment in the porosity of the mortar. Moreover, the data demonstrates that the chloride migration coefficient diminishes as the curing time progresses. This reduction

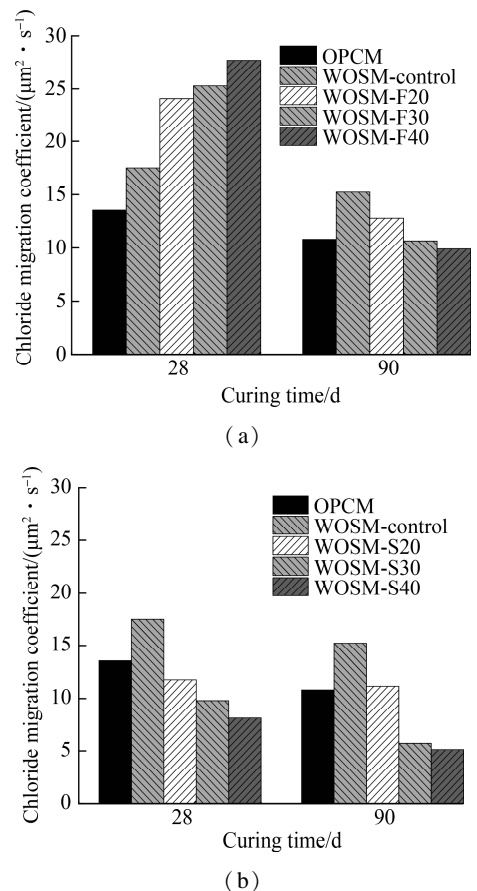


**Fig. 7** Variations in the chloride migration coefficient of WOS mortars with FA and SG. (a) FA; (b) SG

can primarily be ascribed to the sufficient hydration reaction, leading to the heightened internal compactness of WOS mortar and an enhanced antierosion capability<sup>[15]</sup>.

Simultaneously, Fig. 7 indicates that the optimal FA and SG content rests at 30%, and any further elevation in the substitution ratio yields minimal enhancement of chloride diffusion resistance. This observation underscores the robust efficiency of FA and SG in thwarting chloride migration into the mortar<sup>[16]</sup>. Based on these results, SG is more conducive than FA for reducing the chloride migration coefficient of WOS mortar.

## 2.4 Ecological and economic benefits

Concerning environmental implications, CO<sub>2</sub> exhibits the most rapid growth rate as the principal greenhouse gas, and its incessant escalation impacts the climatic conditions of the environment. The sustainability of cementitious materials is principally contingent upon the energy consumption and CO<sub>2</sub> emitted during the manufacturing process. In the present study, the ecological and economic benefits of WOS mortars are assessed by evaluating the

energy consumption ( $E_e$ ) and CO<sub>2</sub> emission ( $E_{CO_2}$ ), with the values of the raw materials summarized in Tab. 3<sup>[17-18]</sup>. Fig. 8 depicts the aggregate  $E_e$  consumed and  $E_{CO_2}$  released for WOS mortars. As observed, the total  $E_e$  and  $E_{CO_2}$  for WOS mortars with FA/SG were remarkably lower in comparison to WOS-Control mortar. This reduction can predominantly be attributed to the substitution of cement with mineral admixtures, which considerably decreases both the  $E_e$  and  $E_{CO_2}$  of the WOS mortar. Furthermore, WOS mortar with 40% FA emerges as the most ecologically friendly mixture, with the  $E_e$  and  $E_{CO_2}$  decreasing by approximately 36.61% and 38.61%, respectively, compared to WOS-control mortar. Moreover, WOS mortar with 40% FA emits the least CO<sub>2</sub>, suggesting that the per unit CO<sub>2</sub> emissions for FA are less than those for SG. Consequently, when 30% of cement is replaced by FA/SG, CO<sub>2</sub> emissions can be curtailed by up to 29% (see Fig. 8). Therefore, WOS mortar with 30% FA/SG may be regarded as a more ecofriendly alternative.

**Tab. 3**  $E_e$  and  $E_{CO_2}$  for the raw materials

Material	Cement	River sand	WOS	Water	Water reducer	FA	SG
$E_e/(MJ \cdot kg^{-1})$	4.800	0.081	0.090	0.200	11.500	0.100	1.600
$E_{CO_2}/(kg \cdot kg^{-1})$	0.767	0.003	0.002	0	0.620	0.019	0.083

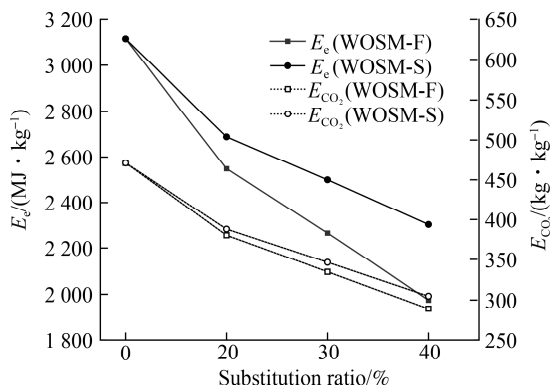


**Fig. 8** Total  $E_e$  consumed and  $E_{CO_2}$  released of WOS mortar

## 3 Conclusions

1) Corresponding to the escalation of FA/SG content, there was an augmentation in the initial slump flow of WOS mortar. This trend signifies that the inclusion of FA/SG considerably enhances the workability of WOS mortars. Consequently, the advised substitution ratio of FA stands at 40%.

2) In terms of mechanical properties, the WOS mortars with FA/SG were inferior to the control mortars at the 28-d interval. However, concurrent with the increasing curing period, the WOS mortars infused with FA/SG exhibited a more pronounced growth rate for compressive strength. Additionally, the mechanical attributes of the WOS mortar with the SG surpassed those with FA, impl-

ying that the recommended substitution ratio for both FA and SG is 30%.

3) The examination of chloride diffusion resistance reveals that as the FA/SG substitution ratio amplifies, there is an increase in the resistance of WOS mortar to chloride diffusion, coupled with a diminution in drying shrinkage. Simultaneously, SG was found to be more efficacious in augmenting durability than FA. This observation further underscores that a 30% replacement of FA/SG results in a substantial improvement.

4) Regarding the environmental footprint, the CO<sub>2</sub> emissions from WOS mortars combined with FA and SG were remarkably less than those of the control mortars. Considering the workability, mechanical properties, and durability of WOS mortars, we can conclude that a 30% FA/SG substitution ratio is an appropriate and advantageous alternative.

## References

- [1] Liu C, Qian R S, Liu Z Y, et al. Multi-scale modelling of thermal conductivity of phase change material/recycled cement paste incorporated cement-based composite material[J]. *Materials & Design*, 2020, **191**: 108646. DOI: 10.1016/j.matdes.2020.108646.
- [2] Mi R J, Pan G H. Slowing down CO<sub>2</sub> effective diffusion speeds in recycled aggregate concrete by using carbon capture technology and high-quality recycled aggregate [J]. *Journal of Building Engineering*, 2022, **45**: 103628. DOI: 10.1016/j.job.2021.103628.

- [3] Eziefula U G, Ezech J C, Eziefula B I. Properties of sea-shell aggregate concrete: A review[J]. *Construction and Building Materials*, 2018, **192**: 287 – 300. DOI: 10.1016/j.conbuildmat.2018.10.096.
- [4] Kuo W T, Wang H Y, Shu C Y, et al. Engineering properties of controlled low-strength materials containing waste oyster shells[J]. *Construction and Building Materials*, 2013, **46**: 128 – 133. DOI: 10.1016/j.conbuildmat.2013.04.020.
- [5] Da B, Yu H F, Ma H Y, et al. Effect of carbonation-drying-wetting on durability of coral aggregate seawater concrete [J]. *Journal of Southeast University*, 2021, **37**(1): 67 – 74. DOI: 10.3969/j.issn.1003-7985.2021.01.009.
- [6] Wang P G, Mo R, Li S, et al. A chemo-damage-transport model for chloride ions diffusion in cement-based materials: Combined effects of sulfate attack and temperature [J]. *Construction and Building Materials*, 2021, **288**: 123121. DOI: 10.1016/j.conbuildmat.2021.123121.
- [7] Jin Z Q, Zhao T J, Gao S, et al. Chloride ion penetration into concrete under hydraulic pressure[J]. *Journal of Central South University*, 2013, **20**(12): 3723 – 3728. DOI: 10.1007/s11771-013-1900-5.
- [8] Liu R W, Chen D, Cai X L, et al. Hardened properties of mortar mixtures containing pre-treated waste oyster shells[J]. *Journal of Cleaner Production*, 2020, **266**: 121729. DOI: 10.1016/j.jclepro.2020.121729.
- [9] Laskar A I, Talukdar S. Rheological behavior of high performance concrete with mineral admixtures and their blending [J]. *Construction and Building Materials*, 2008, **22**(12): 2345 – 2354. DOI: 10.1016/j.conbuildmat.2007.10.004.
- [10] Zhang Y J, Zhang X. Grey connection analysis between particle size distribution of slag powder and fluidity of its cement mortar [J]. *Journal of Tongji University*, 2003, **12**: 1449 – 1453. DOI: 10.3321/j.issn:0253-374X.2003.12.014. (in Chinese)
- [11] Mo K H, Ling T C, Alengaram U J, et al. Overview of supplementary cementitious materials usage in lightweight aggregate concrete [J]. *Construction and Building Materials*, 2017, **139**: 403 – 418. DOI: 10.1016/j.conbuildmat.2017.02.081.
- [12] Zhou S X, Chen Y M, Zhang W S. Prediction of compressive strength of cement mortars with fly ash and activated coal gangue [J]. *Journal of Southeast University (English Edition)*, 2006, **22**(4): 549 – 552. DOI: 10.3969/j.issn.1003-7985.2006.04.022.
- [13] Gesoğlu M, Özbay E. Effects of mineral admixtures on fresh and hardened properties of self-compacting concretes: Binary, ternary and quaternary systems[J]. *Materials and Structures*, 2007, **40**(9): 923 – 937. DOI: 10.1617/s11527-007-9242-0.
- [14] Liu L, Wang X C, Chen H S, et al. Microstructure-based modelling of drying shrinkage and microcracking of cement paste at high relative humidity [J]. *Construction and Building Materials*, 2016, **126**: 410 – 425. DOI: 10.1016/j.conbuildmat.2016.09.066.
- [15] Yu B, Ma Q, Huang H C, et al. Probabilistic prediction model for chloride diffusion coefficient of concrete in terms of material parameters[J]. *Construction and Building Materials*, 2019, **215**: 941 – 957. DOI: 10.1016/j.conbuildmat.2019.04.147.
- [16] Zhao P, Zhou L L, Bai M, et al. Improving chloride ion penetration resistance of cement mortar by strong base anion exchange resin[J]. *Construction and Building Materials*, 2019, **226**: 483 – 491. DOI: 10.1016/j.conbuildmat.2019.07.282.
- [17] Chen D, Zhang P C, Pan T, et al. Evaluation of the eco-friendly crushed waste oyster shell mortars containing supplementary cementitious materials[J]. *Journal of Cleaner Production*, 2019, **237**: 117811. DOI: 10.1016/j.jclepro.2019.117811.
- [18] Mithun B M, Narasimhan M C. Performance of alkali activated slag concrete mixes incorporating copper slag as fine aggregate[J]. *Journal of Cleaner Production*, 2016, **112**: 837 – 844. DOI: 10.1016/j.jclepro.2015.06.026.

## 矿物掺合料对废弃贝壳砂浆的力学性能和耐久性的影响

廖迎娣<sup>1,2,3</sup> 王鑫<sup>1</sup> 封嘉蕊<sup>1,4</sup> 孟彦廷<sup>1</sup> 陈达<sup>1,2,3</sup> 达波<sup>1,2,3</sup>

<sup>(1)</sup> 河海大学港口海岸与近海工程学院, 南京 210098)

<sup>(2)</sup> 河海大学海岸灾害及防护教育部重点实验室, 南京 210098)

<sup>(3)</sup> 河海大学长江保护与绿色发展研究院, 南京 210098)

<sup>(4)</sup> 南京瑞迪高新技术有限公司, 南京 210024)

**摘要:**为有效减少水产养殖废弃物对环境的污染,研究了破碎废弃贝壳(WOS)作为砂浆骨料的可行性.分析了粉煤灰(FA)/矿渣(SG)质量分数(0%、20%、30%、40%)和养护龄期对WOS砂浆的工作性能、力学性能和耐久性的影响,探讨了WOS砂浆的生态经济效益.结果表明:在养护初期阶段,添加矿物掺合料WOS砂浆的抗压强度和静弹性模量略有降低,但是随着养护龄期的增长,WOS砂浆的力学性能有所改善;利用FA/SG取代部分水泥,可有效提高WOS砂浆的抗氯离子渗透性能,降低其干缩率;在满足工程应用要求的前提下,使用WOS砂浆可有效减少CO<sub>2</sub>排放约29%.

**关键词:**废弃贝壳砂浆;工作性能;力学性能;耐久性;生态经济效益

**中图分类号:**TU528